Journal of Great Lakes Research xxx (2017) xxx–xxx

Contents lists available at ScienceDirect

Journal of Great Lakes Research

journal homepage: www.elsevier.com/locate/jglr

Effects of tow transit on the efficacy of the Chicago Sanitary and Ship Canal Electric Dispersal Barrier System

Jeremiah J. Davis [a,*], Jessica Z. LeRoy [b], Matthew R. Shanks [c], P. Ryan Jackson [b], Frank L. Engel [d], Elizabeth A. Murphy [b], Carey L. Baxter [e], Jonathan C. Trovillion [e], Michael K. McInerney [e], Nicholas A. Barkowski [c]

[a] U.S. Fish and Wildlife Service, Carterville Fish and Wildlife Conservation Office, Wilmington Substation, Wilmington, IL, United States
[b] U.S. Geological Survey, Illinois-Iowa Water Science Center, Urbana, IL, United States
[c] U.S. Army Corps of Engineers, Chicago District, Chicago, IL, United States
[d] U.S. Geological Survey, Texas Water Science Center, South Texas Program Office, San Antonio, TX, United States
[e] U.S. Army Corps of Engineers, Engineer Research & Development Center, Construction Engineering Research Lab, Champaign, IL, United States

ARTICLE INFO

Article history:
Received 1 May 2017
Accepted 14 August 2017
Available online xxxx

Associate Editor: Stephen Charles Riley

Keywords:
Asian carp
Barge
Hydraulics
Illinois Waterway
Electric Dispersal Barrier System

ABSTRACT

In 2016, the U.S. Fish and Wildlife Service, U.S. Geological Survey, and U.S. Army Corps of Engineers undertook a field study in the Chicago Sanitary and Ship Canal near Romeoville, Illinois to determine the influence of tow transit on the efficacy of the Electric Dispersal Barrier System (EDBS) in preventing the passage of juvenile fish (total length < 100 millimeters (mm)). Dual-frequency identification sonar data showed that large schools of juvenile fish (mean school size of 120 fish; n = 19) moved *upstream* and crossed the electric field of an array in the EDBS concurrent with downstream-bound (downbound) loaded tows in 89.5% of trials. Smaller schools of juvenile fish (mean school size of 98 fish; n = 15) moved *downstream* and crossed the electric field of an array in the EDBS concurrent with upstream-bound (upbound) loaded tows in 73.3% of trials. Observed fish passages through the EDBS were always opposite to the direction of tow movement, and not associated with propeller wash. These schools were not observed to breach the EDBS in the absence of a tow and showed no signs of incapacitation in the barrier during tow passage. Loaded tows transiting the EDBS create a return current of water flowing between the tow and the canal wall that typically travels opposite the direction of tow movement, and cause a decrease in the voltage gradient of the barrier of up to 88%. Return currents and decreases in voltage gradients induced by tow passage likely contributed to the observed fish passage through the EDBS. The efficacy of the EDBS in preventing the passage of small, wild fish is compromised while tows are moving across the barrier system. In particular, downbound tows moving through the EDBS create a pathway for the upstream movement of small fish, and therefore may increase the risk of transfer of invasive fishes from the Mississippi River Basin to the Great Lakes Basin.

Published by Elsevier B.V. on behalf of International Association for Great Lakes Research.

Introduction

A substantial pathway for the movement of invasive fishes between the Mississippi River Basin and the Great Lakes Basin is the Chicago Area Waterways System (CAWS), including the Chicago Sanitary and Ship Canal (CSSC) in the Upper Illinois Waterway (Asian Carp Regional Coordinating Committee (ACRCC) Monitoring and Rapid Response Workgroup, 2013; U.S. Army Corps of Engineers, 2014). An Electric Dispersal Barrier System (EDBS) was constructed in the CSSC to prevent the movement of invasive fish species between the Mississippi River Basin and the Great Lakes Basin while maintaining the continuity of this important shipping route (Moy et al., 2011). The recent finding of juvenile bigheaded carps (bighead carp *Hypophthalmichthys nobilis*, and silver carp *Hypophthalmichthys molitrix*) further upstream in the Illinois Waterway in the Marseilles Pool near River Mile (RM) 256.6 (ACRCC Monitoring and Response Workgroup, 2015 underscores the need for a complete understanding of the mechanisms that potentially allow fish passage across the EDBS. Therefore, the purpose of this study is to build on existing research addressing the impact of commercial barge traffic (hereafter referred to as tows) on the efficacy of the EDBS in preventing fish passage through a series of field experiments carried out by a multidisciplinary team of scientists and engineers from the U.S. Fish and Wildlife Service (USFWS), the U.S. Geological Survey (USGS), and the U.S. Army Corps of Engineers (USACE).

Previous studies designed to test the efficacy of the EDBS in preventing fish passage have primarily focused on the entrainment and transport of fish in the interstitial spaces between barges. Laboratory experiments in a scaled physical model of the EDBS (Bryant et al., 2016), and field trials conducted at the EDBS (Davis et al., 2016), both

* Corresponding author.
E-mail address: Jeremiah_Davis@fws.gov (J.J. Davis).

http://dx.doi.org/10.1016/j.jglr.2017.08.013
0380-1330/Published by Elsevier B.V. on behalf of International Association for Great Lakes Research.

showed that small fish may be entrained within the gap space formed at the junction between the curved bow of a rake-style barge and the square stern of a box-style barge (rake-to-box junction gaps), and transported in the direction of tow travel. During the field trials, freely-swimming golden shiners (*Notemigonus crysoleucas*) (total length (TL) < 123 mm) in the rake-to-box junction gap showed no signs of harm or incapacitation as the tow transited distances up to 15.5 kilometers (km), through locks, and across the EDBS (Davis et al., 2016). Other research has highlighted the influence of loaded, steel-hulled barges on the voltage gradient in the EDBS, following early suggestions that barges may distort the barrier's electric field (Dettmers et al., 2005). Field tests indicated that the subaqueous electric field within the rake-to-box junction gap between barges was reduced to the point of being "barely measurable" (0.06 volts per centimeter (V/cm) (U.S. Army Corps of Engineers, 2013).

It is well established that loaded tows transiting through confined channels, such as the CSSC, generate a flow of water that moves opposite to the direction of tow travel, hereafter referred to as a "return current" (e.g. Constantine, 1960; Bhowmik et al., 1995; Hochstein and Adams, 1989; Stockstill and Berger, 2001; Das et al., 2012; Bryant et al., 2016). However, the combined effects of tow-induced return currents and electric field distortion on the efficacy of the EDBS in preventing fish passage have not previously been examined in a comprehensive manner at the field scale. The present study addresses this research gap through synchronized sonar observations of wild freely-swimming fish, measurements of flow velocity, and measurements of voltage gradient during upstream-bound (upbound) and downstream-bound (downbound) transits of a loaded tow through the EDBS.

Methods

Study site

This study was conducted during August 2016 in the CSSC at the USACE EDBS, located at RM 296 of the Illinois Waterway, near Romeoville, Illinois, USA (Fig. 1). The CSSC is a confined channel at this location, with a depth of approximately 7.5 meters (m) and width of approximately 48.8 m. The EDBS comprises the Demonstration Barrier (constructed in 2002), Barrier IIB (constructed in 2011), and Barrier IIA (constructed in 2009), listed in order from upstream to downstream (Fig. 1). Barriers IIA and IIB are composed of a high voltage gradient narrow electrode array and a low voltage gradient wide electrode array

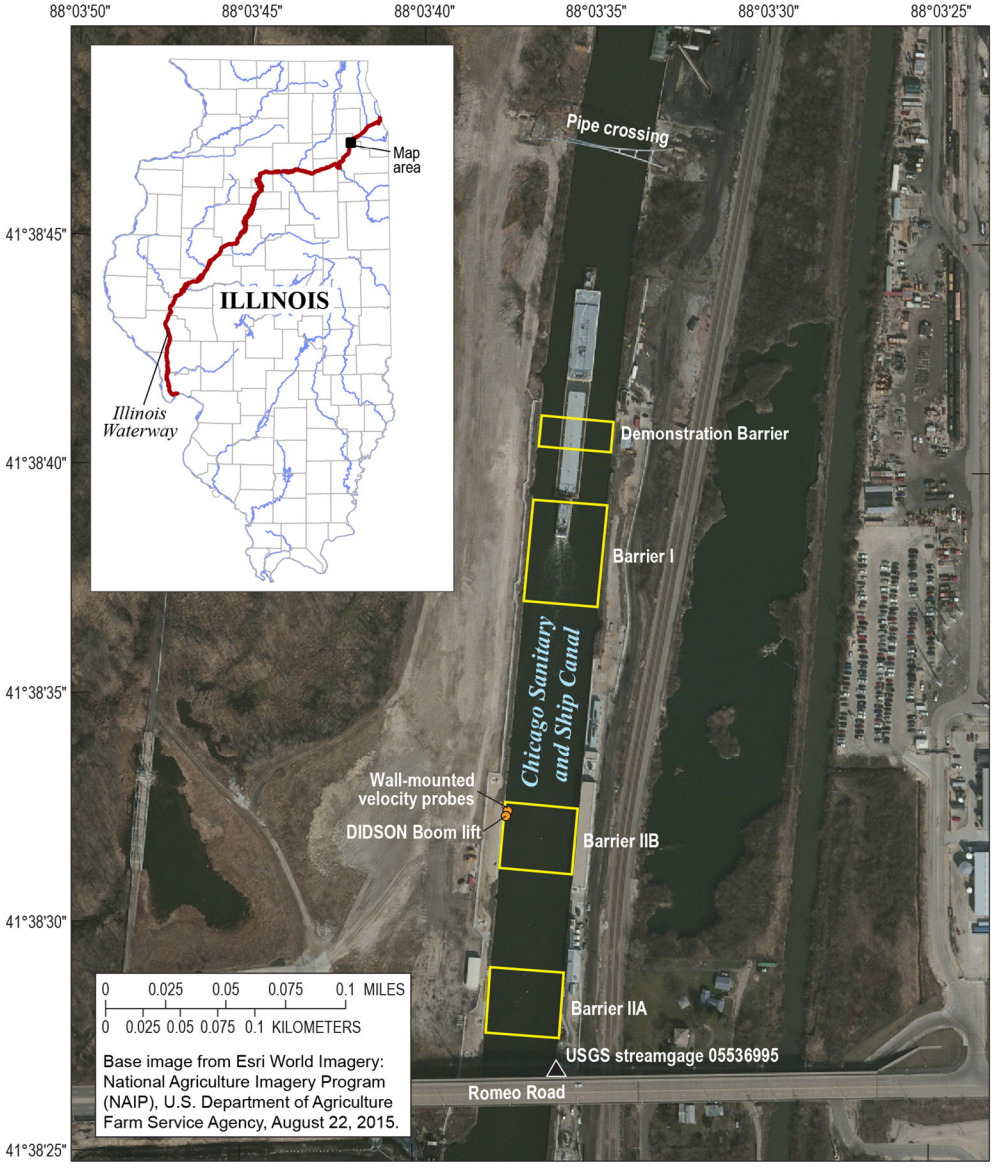

Fig. 1. Location map with annotations showing details of the Electric Dispersal Barrier System.

Please cite this article as: Davis, J.J., et al., Effects of tow transit on the efficacy of the Chicago Sanitary and Ship Canal Electric Dispersal Barrier System, J. Great Lakes Res. (2017), http://dx.doi.org/10.1016/j.jglr.2017.08.013

(hereafter high-field and low-field arrays, respectively). Grids of steel and woven-wire rope, called parasitic structures, are positioned on the bed of the canal upstream of Barrier IIB, between Barriers IIA and IIB, and below Barrier IIA to restrict the extent of the electric field. Barriers IIA and IIB are typically operated to produce nominal voltage gradients of 0.79 V/cm to 0.91 V/cm at the water surface over the high-field array and 0.31 V/cm to 0.39 V/cm at the water surface over the low-field array. The high-field array of each barrier is farther upstream than the low-field array, with each array producing a maximum voltage gradient at the center of the array. Both Barrier IIA (high-field array only) and Barrier IIB (low- and high-field arrays) were energized during the study. During this study, all sonar and electrical data were collected from the western shore of the canal using a boom lift to place the instruments directly over the high-field array of Barrier IIB (Fig. 2). Flow velocity data were collected just upstream of the IIB high-field array (Fig. 2). The water surface elevation at the nearest USGS streamflow-gaging station on the CSSC (Romeoville, Illinois; gage number 05536995; USGS National Water Information System, http://dx.doi.org/10.5066/F7P55KJN) was 175.85 m (North American Vertical Datum of 1988) at 9:15 am Central Daylight Time (CDT) on August 2, 2016 (date of instrument setup), and ranged from 175.477 m to 175.931 m over the study period (August 2 to 11, 2016). Water temperatures were periodically measured during the study by USFWS personnel using a YSI Professional Plus Series Multiparameter Instrument. Observed water temperatures varied between 25.2 °C and 29.7 °C.

Tow configuration and operating protocols

A tow consisting of a tug vessel typical for use on the Illinois Waterway and six fully-loaded barges was contracted for use during this series of experimental trials. The tug vessel was 32.0 m long, had a 9.1-m beam, and drafted 2.3 m. Each of the six 59.4-m by 10.7-m barges held approximately 1360 metric tons of non-hazardous material and drafted 2.7 m. The barges were lashed together in a configuration that was three barges long by two barges wide during all trials (Fig. 3), which is a common configuration for tows in the CSSC (Bryant et al., 2016). During downbound transits, two tow configurations were used, which differed in the position of the rake-to-box junction where instrumentation was located (Fig. 3; blue colors; Electronic Supplementary Material (ESM) Table S1). Rake-style barges were located at the bow of the tow for all upbound transits, and box-style barges were located at the bow of the tow for all downbound transits (Fig. 3; ESM Table S1). While box-style barges are not as common as rake-style barges for the bow of a tow, the magnitude of the return current is governed primarily by the ratio of the channel cross section area to the cross section area of the barge below the waterline (Schijf, 1949). Therefore, the return current magnitude should not vary substantially between a tow with a box or a rake-style barge at the bow. The entire tow package was 210.2 m long and 21.4 m wide, and displaced approximately 11,000 m^3 of water. The length of the tow package relative to the channel width did not allow the entire tow to be turned around in the channel; therefore, only the tug vessel was repositioned to the opposite side of the tow between upbound and downbound trials.

The tow traveled southbound near the channel centerline for downbound transits ($n = 22$), and northbound for upbound transits ($n = 23$). The boundaries of the transit pathway were Romeo Road bridge, located approximately 180 m downstream of the EDBS (Fig. 1; 41.640698 North (N), 88.060169 West (W), World Geodetic System 1984 (WGS84)), and a pipe crossing, located approximately 440 m upstream of the EDBS (Fig. 1; 41.646401 N, 88.059548 W, WGS84). During each transit, the tow would enter the study area traveling at typical operating speeds (1.15 to 1.91 meters per second (m/s); ESM Table S1), pass through the entire EDBS, exit the study area, then decelerate over approximately 100 to 150 m, stop, and moor to the west wall. The

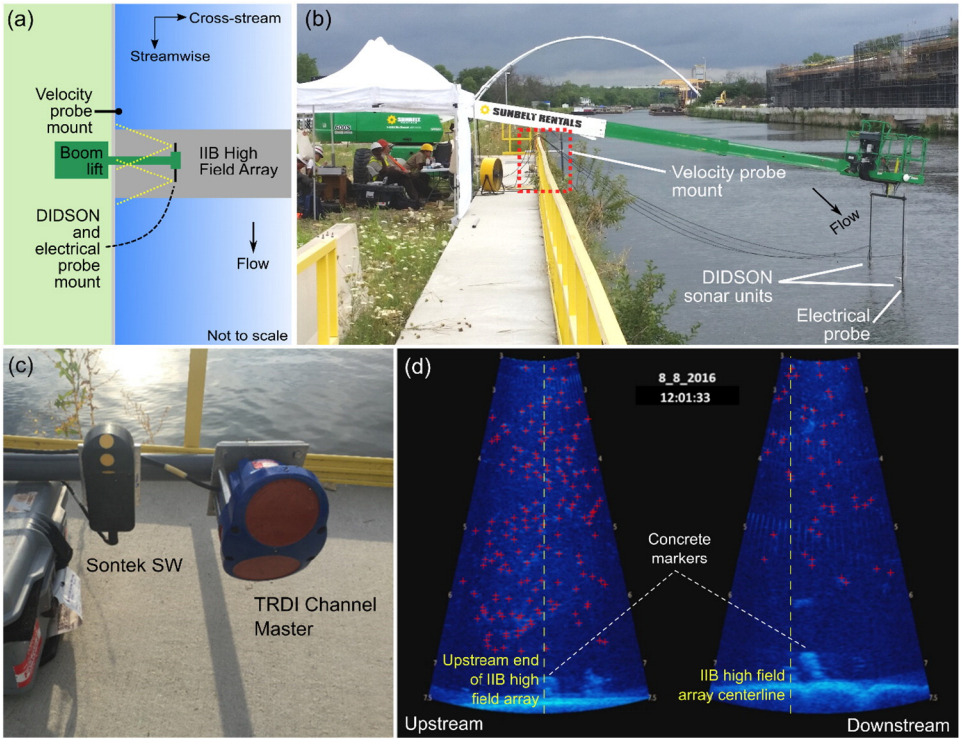

Fig. 2. (a) Sketch of wall-mounted instrument setup (not to scale).Yellow dotted lines roughly denote the area ensonifed by the DIDSON sonars. (b) Photograph of wall-mounted instrument setup showing the telescopic boom lift that deployed two DIDSON multi-beam sonar units in parallel at the Chicago Sanitary and Ship Canal Electric Dispersal Barrier System. View is toward the upstream end of the study area. The white polyvinyl chloride (PVC) housing of the electrical probe is visible near the water surface, above the downstream DIDSON. The velocity probes were mounted upstream of the boom lift (see red dotted box). (c) Sontek SW and Teledyne RDI (TRDI) 600 kHz Channel Master mounted on grey PVC pipe (resting sideways). (d) Example of two parallel DIDSON multi-beam sonar echograms showing fish passage at the Electric Dispersal Barrier System. Red crosshairs denote fish locations on the echograms. (For interpretation of the references to color in this figure legend, the reader is referred to the web version of this article.)

Please cite this article as: Davis, J.J., et al., Effects of tow transit on the efficacy of the Chicago Sanitary and Ship Canal Electric Dispersal Barrier System, J. Great Lakes Res. (2017), http://dx.doi.org/10.1016/j.jglr.2017.08.013

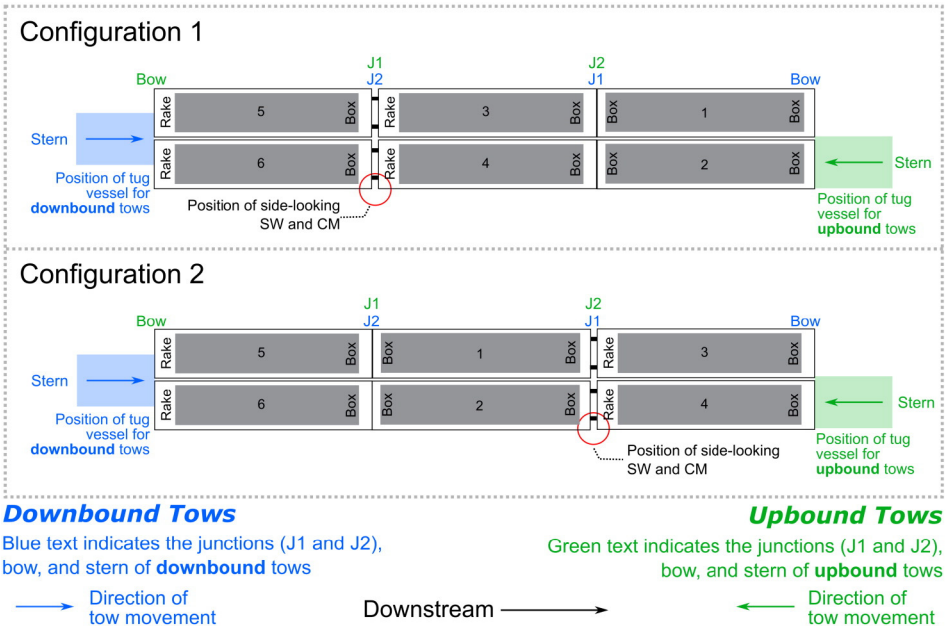

Fig. 3. Tow configurations used during field trials at the Electric Dispersal Barrier System. The side-looking velocity probes (SW and CM) measured water velocity in the area between the tow and the west side of the canal.

distance between the tow and the west canal wall was measured using laser rangefinders and tow-mounted Global Positioning System (GPS) receivers as the bow, barge junctions, and stern of the tow passed over Barrier IIB (ESM Table S1).

Flow velocity measurements

Velocity profiles were measured during upbound and downbound transits through the EDBS using four synchronized tow-mounted and wall-mounted hydroacoustic velocity probes (Figs. 1–3). SonTek Argonaut SW™ 3000 kilohertz (kHz) acoustic Doppler velocity meters (SW) were used in both wall- and tow-mounted configurations, along with a wall-mounted 600 kHz Teledyne RD Instruments Channel Master™ horizontal acoustic Doppler current profiler (CM) and a tow-mounted 1200 kHz CM. During measurement, the SWs and CMs measured velocities for 10 pings every 10 s (SW ping rate = 10 Hz; CM ping rate = 3.33 Hz), then recorded the average of the 10 pings. Due to instrument limitations, water velocity could only be measured in about 85% of the distance between the tow and the canal wall; measurements near the tow and the wall were not possible.

Two side-looking velocity probes, the 600 kHz CM and an SW (Fig. 2c), were mounted on the west canal wall at depths of 1.7 m and 1.4 m, respectively, as measured at 09:15 am CDT on August 2, 2016. The wall-mounted velocity probes were located just upstream from Barrier IIB (Figs. 1 & 2; 41.6423629 N, 88.0603289 W, WGS84). The SW profiled streamwise and cross-stream components of velocity at 10 cells spaced by 0.5 m between 0.57 and 6.07 m from the wall. The 600 kHz CM also measured profiles of streamwise and cross-stream components of velocity, but was capable of profiling the width of the canal when no tows were blocking its acoustic beams (45 cells spaced by 1.0 m starting 2.8 m from the west wall, and extended to 4.0 m from the opposite wall). In addition to measuring water velocity while the test tow transited the EDBS, the wall-mounted SW and CM recorded velocities prior to tow transit which gives an estimation of the ambient flow velocity in the canal for all trials except the first upbound and downbound transits on August 9th, 2016 (ESM Table S1).

The flow field alongside the tow at the position of the rake-to-box junction was measured using an SW and the 1200 kHz CM. Both instruments faced outward from the side of the tow (side-looking SW and CM in Fig. 3) and were placed at a depth of 1.4 m. The 1200 kHz CM and the SW were located at distances of 0.7 m and 0.8 m from the box-side of the gap (measured toward the rake-side of the gap), respectively. The side-looking SW profiled velocity at 10 cells spaced by 0.5 m between −0.47 m and 5.53 m measured perpendicular to the tow side, where the negative sign indicates that the start of the first SW bin was located within the rake-to-box gap. The side-looking 1200 kHz CM was configured to profile velocity at 35 cells spaced by 0.5 m starting at 0.52 m and extending to 18.02 m from the tow. Velocity profiles measured with the tow-mounted CM were terminated at 65% to 93.5% (mean = 85.8%, standard deviation (S.D.) = 6.8%) of the distance between the tow and the wall (as measured at the time the tow-mounted instruments passed over Barrier IIB) during post-processing. A Hemisphere V102™ differential GPS (DGPS) with Doppler-based heading was mounted on the box-side of the rake-to-box junction and synchronized with the side-looking velocity probes. The DGPS provided positions (sub-meter accuracy), heading (accuracy ±0.75°), and speed of the tow at a sampling frequency of 10 Hz.

The time-stamped velocity measurements from the tow-mounted side-lookers were matched to the nearest-in-time DGPS position and corrected for the velocity of the moving tow. Once corrected for the movement of the tow, the velocity data were rotated into the local streamwise-cross-stream coordinate system, such that streamwise velocities are parallel to the banklines of the CSSC and positive downstream, and cross-stream velocities are perpendicular to the banklines and positive toward the east (left-descending) bank. The wall-mounted SW and CM did not require corrections for movement because they were stationary and did not require coordinate rotation because they were mounted parallel to the canal banklines.

The mean return current velocity (as measured by each instrument) was computed for each trial and for each velocity probe by first averaging the streamwise velocity profile measured by the velocity probe over the period of time that the tow passed Barrier IIB, and then spatially averaging the resultant profile over the measured portion of the distance between the tow and the canal wall. Measurement cells located inside the rake-to-box junction gap of the tow or within 1.5 m of the tow side were excluded from the return current calculation to avoid velocities measured in the areas that are influenced by the flow structure of the rake-to-box junction gap (Davis et al., 2016) or the tow boundary layer (Bryant et al., 2016).

Please cite this article as: Davis, J.J., et al., Effects of tow transit on the efficacy of the Chicago Sanitary and Ship Canal Electric Dispersal Barrier System, J. Great Lakes Res. (2017), http://dx.doi.org/10.1016/j.jglr.2017.08.013

The observed return currents are influenced by the magnitude of the ambient flow in the canal which varied during the field experiments due to lock and dam operations and natural hydrologic variations (Jackson et al., 2012). The ambient streamwise flow velocity was calculated as the cross-sectional average streamwise velocity measured by the wall-mounted CM, averaged over 5 to 10 min prior to tow transit through the EDBS (ESM Table S1). The return currents corrected for ambient flow velocity are computed by subtracting the ambient flow velocity in the canal from the observed mean return currents.

Multi-beam sonar

A mobile telescopic boom lift was used to deploy two Sound Metrics Dual-frequency identification sonar (DIDSON) 300M™ multi-beam systems into the canal from the western canal bank (Fig. 2). Custom mounts attached the two sonar systems to the cage at the end of the boom, spaced 3.7 m apart. The two sonar systems were always deployed 0.3 m below the water surface, parallel to the western canal wall, and aimed toward the western wall. The distance from the western wall to the sonar systems ranged from 4.3 to 7.0 m, which was the farthest distance from the western wall that the DIDSON units could be placed without risking a collision with the moving tow. This configuration allowed acoustic coverage of the majority of the streamwise width of the Barrier IIB high-field array at the canal wall. The two sonar units were synchronized and simultaneously operated from one computer in identification mode with 96 acoustic beams that produced a 29° acoustic cone at 1.8 MHz. The receiver gain was 40 dB, and the data collection frame rate was 8 frames per second.

Concrete reference markers were placed on the wall, below the water surface, at the upstream and downstream boundaries of the Barrier IIB high-field array and at the point of maximum voltage gradient, so that accurate positioning of the sonar system could be maintained. The sonar systems were positioned so that the upstream reference marker was detected by the upstream sonar unit, and the maximum electrical field strength marker was detected by both upstream and downstream sonar units.

Sonar data were recorded continuously during 15 of the 23 upbound transits and 19 of the 22 downbound transits. Sonar data collection began before the tow entered the EDBS restricted navigation area and concluded after the tow exited the restricted navigation area (mean data collection period = 9 min 20 s). Sonar data were post-processed and reviewed in the laboratory. Three independent readers enumerated the number of wild fish that challenged or breached the high-field array at Barrier IIB, and the reader results were averaged (Fig. 2d). A breach, or passage, was considered to have occurred when fish were observed swimming past the reference marker denoting the point of greatest electrical field strength and then continuing to swim in the same direction across the entire upstream or downstream sonar field of view. Note that any fish observed moving upstream across the Barrier IIB high-field array must have crossed the low-field array to reach the area observed with the sonar systems. The lengths of a subsample of fish (n = 10) from each trial were also measured using the measurement tool in the DIDSON V5.25™ software.

Electrical measurements

Three-dimensional (streamwise, cross-stream, and vertical) voltage gradient measurements were collected with a Pacific Instruments Series 6800 ICP Data Acquisition System Model 6825-24 using Pacific Instruments PI660-6000 Version 9.000 release 2.078 software. Electrode pairs for each axis were connected to a non-conductive polyvinyl chloride (PVC) frame with an electrode spacing of 63.5 cm to form a 3-dimensional probe. Test Products International differential probes Model ADF25 were used between the electrode pairs and the Pacific Instruments system to attenuate the input voltage and provide electrical isolation. Electrical data were collected at a sampling rate of 8 kHz which is sufficient to resolve the individual barrier pulses. Data analysis focused on the component of the voltage gradient that is parallel to the streamwise direction, as it is the primary voltage gradient component affecting fish behavior in the absence of a tow (Holliman et al., 2015).

During most runs (n = 34), the PVC electric field probe was placed directly underneath the downstream DIDSON sonar unit at a depth of 0.5 m and mounted to the isolated steel fixture fabricated for DIDSON sonar sampling. The electric field probe was located at the canal wall for all other measured runs (n = 9), and two runs did not include any electric field measurement (ESM Table S1). Electrical field measurements were reviewed for data quality following the trials, and data sets with poor GPS timing synchronization or electrical data were discarded. This quality control screening resulted in 7 trials where the electrical field probe was located along the canal wall and 30 trials when the probe was co-located with the DIDSON units. Data from both mounting positions were combined for all analyses.

A 60-s electric field measurement was recorded at the beginning and end of each day. Electrical measurements during each transit of the EDBS were recorded for the period of time that the tow was within the study area described above. Time stamps were recorded at the start and stop times of electrical data collection, as well as the times that the bow of the tow, the 1st barge junction, the 2nd barge junction, center of second barge, the barge and tug vessel junction, and the stern of the tug vessel (Fig. 3) passed over the center of the Barrier IIB narrow array. Unformatted binary files from the PI660-6000 software were analyzed using DPLOT Version 2.3.2.6 software (developed by HydeSoft Computing LLC). The voltage gradients at each time stamp, and the minimum voltage gradient during each run, were determined by analyzing individual electrical pulses and determining a maximum pulse value (ESM Table S1). Additionally, the voltage gradient at the beginning and end of each run were averaged to determine a mean baseline voltage gradient for each run.

GPS data collection and processing

In addition to the DGPS used for flow velocity data analysis, five GPS data collection devices were deployed throughout the trials. A Trimble GeoXH6000™ with a Zephyr™ external antenna was attached to the boom lift to record the location of the electrical probe at a sampling rate of 2 Hz. A Trimble GeoXH2008™, and three OHARARP LLC SD GPS Data Logger V3.15™ devices were deployed along the streamwise axis of the tow. The locations of the GPS units on the tow were mapped relative to the bow, stern, and sides of the barges. The GPS units were positioned in the same location on the tow each day during the study. All GPS units continuously recorded tracklog data at a sampling rate of at least 0.5 Hz for each day of testing and timestamped samples using data embedded in the GPS satellite signal. The GPS data were analyzed in ESRI ArcGIS™ software to determine the position of the tow, the angle of the tow, and the perpendicular distance from the tow to the electrical field probe and the canal wall at each time stamp of interest.

Wild fish sampling

Targeted wild fish sampling downstream of the EDBS was conducted during the field trials, because the species of fish observed cannot be determined using the multi-beam sonar system. The fish collection vessel conducted targeted electrofishing passes within the CSSC immediately downstream of Barrier IIB and upstream of the narrow array of Barrier IIA following standard Long Term Resource Monitoring Program electrofishing protocols (Ratcliff et al., 2014, pp. 14–15). These fish collections used a boat-mounted Smith-Root 7.5 GPP™ DC electrofisher operating at 60 pulses per second and 80% of range, with an output from 16 to 20 amps. All fish specimens collected were identified to species and measured (total length, TL) to determine the species composition of the fish community near the EDBS.

Please cite this article as: Davis, J.J., et al., Effects of tow transit on the efficacy of the Chicago Sanitary and Ship Canal Electric Dispersal Barrier System, J. Great Lakes Res. (2017), http://dx.doi.org/10.1016/j.jglr.2017.08.013

Results

Velocity measurements

Two representative trials, a downbound transit on August 8, 2016 and an upbound transit on August 8, 2016, were selected to illustrate the observed patterns in streamwise flow velocity which were remarkably similar across trials ($n_{downbound} = 22$, $n_{upbound} = 23$). The time-series of streamwise velocities measured by the wall-mounted CM (located near Barrier IIB, Figs. 1 & 2) demonstrates the influence of the moving tow on the flow velocities in the canal during the downbound transit on August 8, 2016 (Fig. 4a) (see LeRoy et al., 2017 for complete time-series datasets). Prior to passage of the downbound tow, the streamwise velocities measured by the wall-mounted CM were positive (downstream), and represented ambient flow conditions. As the bow of the downbound tow passed the wall-mounted instruments, the streamwise velocities between the tow and the west canal wall rapidly decreased and became negative (upstream) for the duration of tow passage. In contrast, during the upbound transit on August 8, 2016, the movement of the tow past the wall-mounted instruments coincided with a substantial increase in the streamwise velocity relative to the ambient flow conditions (Fig. 4b). The return current is defined herein as the velocity measured between the tow and the canal wall during the period of time the tow is passing the wall-mounted instruments. After the tow passed the wall-mounted instruments, the streamwise velocities were influenced by the propeller wash from the tug vessel, but began to return to normal downstream flow conditions as the tow moved out of the study area for both the downbound and upbound transits (Fig. 4).

The time-averaged return current profile for the downbound transit on August 8, 2016 shows upstream flow over most of the measured distance between the tow and the west canal wall, though water is moving downstream (with the tow) inside and near the rake-to-box junction gap (e.g. Davis et al., 2016; Fig. 5a). The opposite is found for the upbound transit, in which the water is moving downstream between the tow and the west canal wall, and upstream (with the tow) inside the rake-to-box junction gap (Fig. 5b). There is good agreement between the time-averaged return current profiles measured by the individual velocity probes for both of the selected downbound and upbound transits (Fig. 5). Small discrepancies between the return current computed for the different instruments may result from the different measurement volumes of the instruments (e.g. the SWs measure over a shorter distance and have a different beam angle than the CMs), and/or differences between the amount of processing required for the wall-mounted and the tow-mounted instruments. The return current velocities computed from the individual velocity probe measurements (ESM Tables S2 and S3) were averaged to give an estimation of the mean return current velocity for these two runs (Downstream Run 1

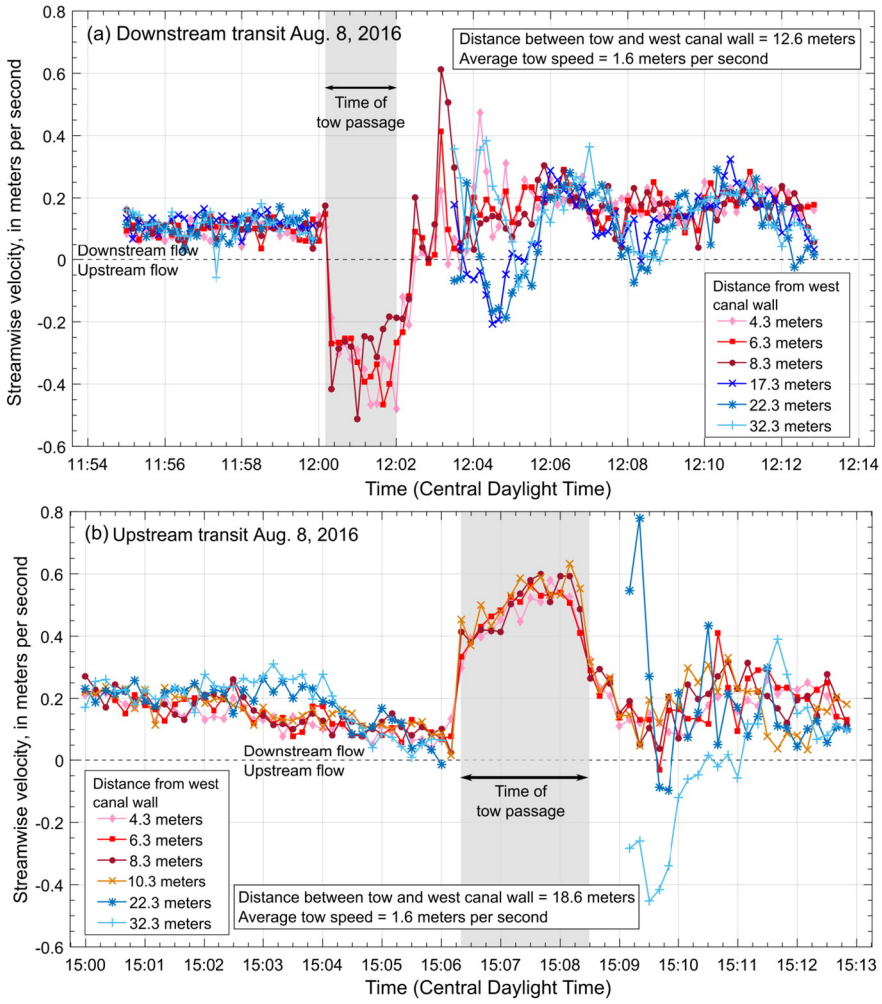

Fig. 4. Time-series of streamwise velocities measured by the wall-mounted Channel Master at selected measurement cells during (a) a downbound transit, and (b) an upbound transit on August 8th, 2016. Positive streamwise velocities indicate downstream flow, and negative streamwise velocities indicate upstream flow. The shaded grey bar indicates the period of time during which the tow passed the wall-mounted instruments (near Barrier IIB). Note that measurement cells shown with blue colors were far enough from the west canal wall that the tow blocked the acoustic beam of the wall-mounted Channel Master as it passed the instrument, whereas the cells shown with red colors were located between the tow and the west canal wall. (For interpretation of the references to color in this figure legend, the reader is referred to the web version of this article.)

Please cite this article as: Davis, J.J., et al., Effects of tow transit on the efficacy of the Chicago Sanitary and Ship Canal Electric Dispersal Barrier System, J. Great Lakes Res. (2017), http://dx.doi.org/10.1016/j.jglr.2017.08.013

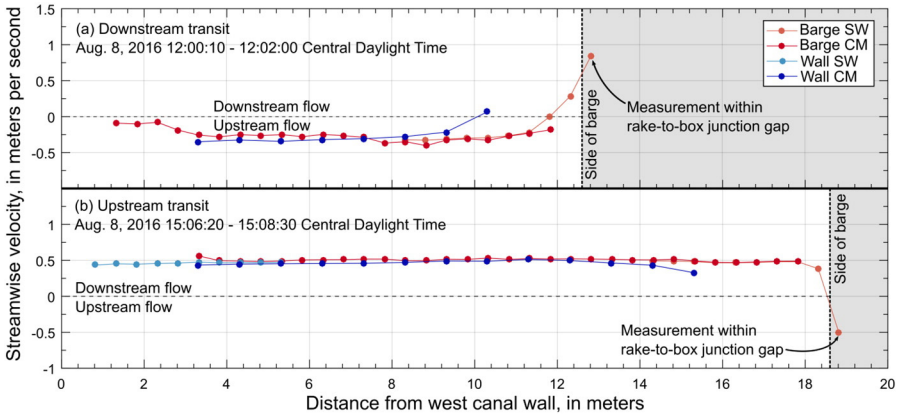

Fig. 5. Time-averaged return current profiles for the (a) downbound transit (no wall-mounted SW data were available for this transit), and (b) upbound transit on August 8th, 2016, that are shown in Figs. 3 and 4. The velocities shown were averaged over the period of time during which the tow passed the wall-mounted instruments (downbound transit: 12:00:10 to 12:02:00 Central Daylight Time (CDT), and upbound transit 15:06:20 to 15:08:30 CDT). Note that one of the measurement cells of the barge-mounted SW is located within the rake-to-box junction gap of the tow.

and Upstream Run 3) on August 8, 2016. The mean return current velocity for the downbound transit was −0.24 m/s (S.D. = 0.06 m/s, $n_{ADVMs} = 3$), and for the upbound transit was 0.44 m/s (S.D. = 0.05 m/s, $n_{ADVMs} = 4$).

The two August 8, 2016 transits described above are representative examples of the return currents measured during the downbound and upbound trials (ESM Tables S2 and S3). An increase in streamwise velocities between the tow and the canal wall occurred for all upbound trials, and a decrease in streamwise velocities, typically to the point of flow reversal, between the tow and the canal wall occurred for all downbound trials. Descriptive statistics for the return current velocities were calculated from the average of the return current velocities determined from the four instruments (Table 1, and ESM Tables S2 and S3). The mean observed return current velocity for downbound tows was −0.12 m/s (S.D. = 0.08 m/s, $n_{downbound} = 22$, and for upbound tows was 0.45 m/s (S.D. = 0.9 m/s, $n_{upbound} = 23$).

The return current is significantly correlated with ambient flow velocity (significance level defined as p-value <0.05) for downbound tows (correlation = 0.63, p = 0.002), but the correlation between return current and ambient flow velocity is not significant for upbound tows (correlation = 0.37, p = 0.095). In one case, the ambient flow velocity (0.33 m/s) was sufficient to maintain downstream flow, as measured by all four velocity probes, during a downbound passage of the tow moving at 1.3 m/s (August 2, 2016, Downstream Run 2; ESM Table S2). Correcting the return current to account for the ambient flow velocity of the water provides an estimation of what the return current would be if the tow was moving through still water. The mean return current corrected for ambient flow velocity for downbound tows was −0.29 m/s (S.D. = 0.07 m/s, $n_{downbound} = 22$), and for upbound tows as 0.31 m/s (S.D. = 0.08 m/s, $n_{upbound} = 23$) (Table 1). Thus, when the influence of the ambient flow velocity is removed, the magnitude of the return current is similar for upbound and downbound tows, and the sign (positive vs. negative) is solely determined by the direction of tow movement relative to the chosen coordinate system. This result validates the theoretical prediction that return currents flow opposite to the direction of vessel movement in still water (Schijf, 1949), and the previous statement that the magnitude of the return current is not strongly dependent on the shape (rake or box) of the bow of the tow.

Electrical measurements

Measured baseline voltage gradients over the high-field array of Barrier IIB averaged 1.04 V/cm (S.D. = 0.02) during this study. The minimum voltage gradient observed during each run ranged from 0.12 to 0.91 V/cm corresponding to an 88% to 12% (mean = 25.88%; S.D. = 14.10; median = 20.42%) reduction from the baseline voltage gradient for each run (ESM Table S1). The minimum voltage gradient always occurred when the barges of the tow were positioned over Barrier IIB, for both upbound and downbound transits. The time at which the center of the second barge passed over the high-field array of Barrier IIB, and was aligned with the voltage gradient probe, was used to analyze trends across runs. There was not a significant difference in maximum percentage of voltage reduction between upbound (mean = 22.10%; S.D. = 16.15; median = 19.18%) and downbound (mean = 29.66%; S.D. = 10.85; median = 27.27%) transits (*t*-test; $t(35) = -1.48$; p = 0.146). Therefore, upbound and downbound transits were combined to analyze the relationship between the distance of the tow from the electrical field probe and the percent reduction in voltage gradient from the baseline value (at the time when the center of the second barge passed the probe). The data were log-transformed and a linear regression was used to predict reduction in voltage gradient based on the distance of the tow from the probe. A significant regression equation was found ($F(1,35) = 69.64$; $p < 0.0001$; $r^2 = 0.67$; n = 37), which predicted a greater percent reduction in voltage gradient when the tow was closer to the probe (Fig. 6).

Table 1
Minimum, maximum, mean, and standard deviation of the return current velocity (as averaged over the four velocity probes for each transit).

Return current velocities Positive = downstream; Negative = upstream	Return current velocities, in meters per second			
	Upstream-bound tows (n = 23)		Downstream-bound tows (n = 22)	
	Observed	Corrected for ambient velocity	Observed	Corrected for ambient velocity
Minimum magnitude	0.36	0.17	0.10	−0.09
Maximum magnitude	0.79	0.61	−0.24	−0.40
Mean	0.45	0.31	−0.12	−0.29
Standard deviation	0.09	0.08	0.08	0.07

Please cite this article as: Davis, J.J., et al., Effects of tow transit on the efficacy of the Chicago Sanitary and Ship Canal Electric Dispersal Barrier System, J. Great Lakes Res. (2017), http://dx.doi.org/10.1016/j.jglr.2017.08.013

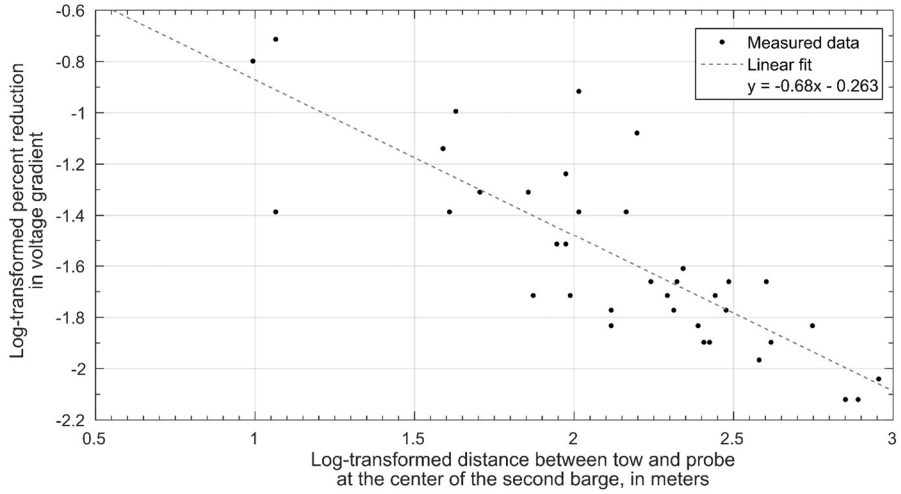

Fig. 6. Log-transformed percent reduction in voltage gradient plotted against the log-transformed distance between the tow and the probe at the center of the second barge (black dots), and the linear fit to the data (dotted line; $R^2 = 0.67$, $P < 0.0001$).

Multi-beam sonar

Multi-beam sonar echograms indicated that fish passage over the high-field array of Barrier IIB occurs concurrently with tow transits. Upstream fish passage across Barrier IIB was concurrent with reductions in the voltage gradient and upstream-flowing return currents induced by downbound transiting tows (Fig. 7). Similarly, downstream fish passage across Barrier IIB coincided with reductions in voltage gradient and downstream-flowing return currents generated by upbound transiting tows (Fig. 8). Fish substantially larger than 100 mm were not observed crossing Barrier IIB. No fish were observed crossing Barrier IIB before or after the transit of a tow during any trial.

Upstream fish passage was observed during 89.5% (n = 19) of downbound tow transit trials (Table 2). The number of fish that achieved complete upstream passage of the EDBS during each trial was highly variable. The number of fish passages observed during each downstream tow transit ranged from 0 to 822 (mean = 120 fish/transit, S.D. = 199; median = 49). Sonar-based size estimates of fish that achieved passage across Barrier IIB ranged from 38 mm to 92 mm (mean = 61.4 mm, S.D. = 7.4). No fish were observed crossing Barrier IIB in the downstream direction during downbound transits. However, schools of small fish were observed moving in the downstream direction over the Barrier IIB high-field array during 73.3% of upbound tow transit trials where sonar data were available (n = 15) (Table 3). The number of fish that moved downstream across the high-field array of Barrier IIB during upstream tow transits ranged from 0 to 528 (mean = 98 fish/transit, S.D. = 139; median = 55). Fish moving through the Barrier IIB high-field array in both the upstream (during downbound transits) and downstream (during upbound transits) direction were visually observed to actively swim at a velocity greater than passive debris moving in the streamwise direction, and to rapidly change direction while swimming. This suggests that some fish were not incapacitated while traversing the Barrier IIB high-field array in either direction.

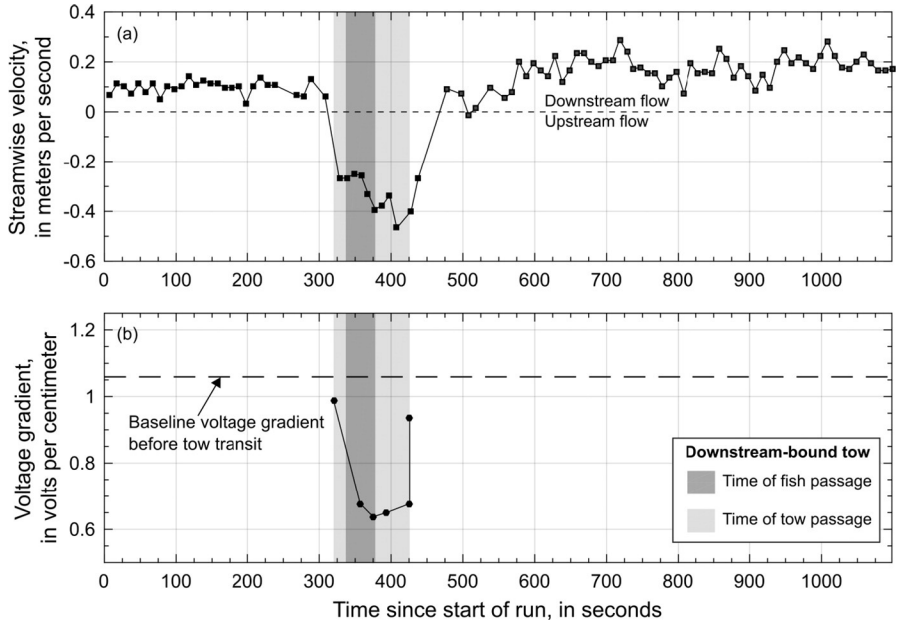

Fig. 7. Velocity and voltage gradient data from a downbound tow transit of the Electric Dispersal Barrier System (EDBS) on August 8th, 2016. As the tow transited EDBS Barrier IIB, reverse flows (negative flow velocity, top panel) were initiated concurrent with substantial reductions in voltage gradient (bottom panel). (a) The streamwise component of velocity was measured 5.3 m from the west wall of the canal. Positive flow velocity indicates downstream flow and negative flow velocity indicates upstream flow. (b) The voltage gradient during tow passage. The light grey shading indicates the time during which six loaded barges passed the DIDSON multi-beam sonar units. The dark grey shading indicates the time during which wild fish were observed fully traversing the EDBS Barrier IIB in the upstream direction.

Please cite this article as: Davis, J.J., et al., Effects of tow transit on the efficacy of the Chicago Sanitary and Ship Canal Electric Dispersal Barrier System, J. Great Lakes Res. (2017), http://dx.doi.org/10.1016/j.jglr.2017.08.013

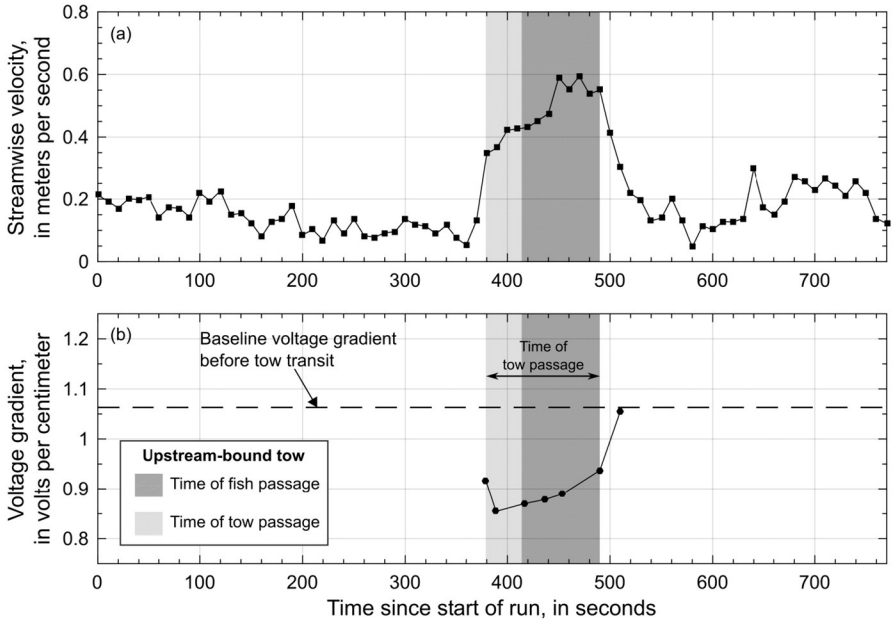

Fig. 8. Velocity and voltage gradient data from an upbound tow transit of the Electric Dispersal Barrier System (EDBS) on August 8th, 2016. As the tow transited EDBS Barrier IIB, the downstream velocity increased concurrent with substantial reductions in voltage gradient (bottom panel). (a) The streamwise component of velocity was measured 5.3 m from the west wall of the canal. Positive flow velocity indicates downstream flow and negative flow velocity indicates upstream flow. (b) The voltage gradient during tow passage. The light grey shading indicates the time during which six loaded barges passed the DIDSON multi-beam sonar units. The dark grey shading indicates the time during which wild fish were observed fully traversing the EDBS Barrier IIB in the downstream direction.

Wild fish sampling

All fish that were physically captured in the area immediately downstream of the EDBS concurrent with tow transit trials were either gizzard shad (*Dorosoma cepedianum*) (n = 304) or threadfin shad (*Dorosoma petenense*) (n = 6). The mean size of physically captured gizzard shad was 54.0 mm (S.D. = 8.95), and of threadfin shad was 53.8 mm (S.D. = 5.54). Gizzard shad sizes ranged from 33 to 94 mm, and threadfin shad ranged in length from 48 to 60 mm.

Discussion

The results of this study indicate that the efficacy of the EDBS in preventing passage of small fish (TL < 100 mm) is compromised while loaded tows are moving across the barrier system. Small fish fully traversed the high-field array Barrier IIB of the EDBS - without becoming incapacitated - within the ensonified area between the DIDSON mount and the west canal wall during both upbound and downbound tow transits. The observed fish passage across the barrier is likely

Table 2
Number of upstream fish passages through the Electric Dispersal Barrier System, Barrier IIB high-field array during each downbound tow transit. The average number of fish passages and standard deviation (S.D.) for the three independent readers are shown. Date and run numbers correspond to date and run numbers in ESM Table S1. Mean length is the average of 10 randomly selected fish from each tow transit as measured on sonar echograms. Times are given in Central Daylight Time (CDT); (N/A) not applicable; mm, millimeter; S.D., standard deviation.

Date	Run Number	Time first fish passage (CDT)	Time last fish passage (CDT)	Number of fish passages	S.D. of fish passages	Mean length (mm)	S.D. of mean length (mm)
8/2/2016	Downstream #1	No data	No data	No data	No data	No data	No data
8/2/2016	Downstream #2	N/A	N/A	0	0.00	N/A	N/A
8/3/2016	Downstream #1	15:38:37	15:40:40	66	20.2	61.5	14
8/3/2016	Downstream #2	16:44:18	16:45:27	20	6.7	55.0	8
8/4/2016	Downstream #1	10:05:36	10:06:52	126	18.7	49.8	7
8/4/2016	Downstream #2	11:26:52	11:28:23	29	9.5	48.1	11
8/4/2016	Downstream #3	15:15:42	15:16:15	2	1.0	52.9	22
8/4/2016	Downstream #4	16:32:08	16:33:53	18	11.9	51.7	15
8/5/2016	Downstream #1	No data	No data	No data	No data	No data	No data
8/8/2016	Downstream #1	12:01:09	12:01:50	427	30.4	69.1	8
8/8/2016	Downstream #2	No data	No data	No data	No data	No data	No data
8/8/2016	Downstream #3	N/A	N/A	0	0.00	N/A	N/A
8/8/2016	Downstream #4	16:50:10	16:51:12	75	3.5	62.7	8
8/9/2016	Downstream #1	10:58:07	10:59:49	33	1.5	73.6	11
8/9/2016	Downstream #2	14:53:23	14:54:25	39	6.4	68.4	12
8/9/2016	Downstream #3	16:00:14	16:01:34	140	16. 6	63.6	12
8/10/2016	Downstream #1	10:07:03	10:08:23	227	16.7	61.4	8
8/10/2016	Downstream #2	11:13:44	11:15:00	822	40.1	67.4	8
8/10/2016	Downstream #3	15:00:59	15:02:00	82	10.0	63.6	15
8/10/2016	Downstream #4	16:14:30	16:15:46	49	3.2	67.6	7
8/11/2016	Downstream #1	11:39:25	11:39:46	3	1.0	63.5	13
8/11/2016	Downstream #2	15:40:37	15:41:52	118	9.9	64.2	13

Please cite this article as: Davis, J.J., et al., Effects of tow transit on the efficacy of the Chicago Sanitary and Ship Canal Electric Dispersal Barrier System, J. Great Lakes Res. (2017), http://dx.doi.org/10.1016/j.jglr.2017.08.013

Table 3
Number of downstream fish passages through the Electric Dispersal Barrier System, Barrier IIB high-field array during each upbound tow transit. The average number of fish passages and standard deviation (S.D.) for the three independent readers are shown. Date and run numbers correspond to date and run numbers in ESM Table S1. Mean length is the average of 10 randomly selected fish from each tow transit as measured on sonar echograms. Times are given in Central Daylight Time (CDT); (N/A) not applicable; mm, millimeter; S.D., standard deviation.

Date	Run Number	Time first fish passage (CDT)	Time last fish passage (CDT)	Number of fish passages	S.D. of fish passages	Mean length (mm)	S.D. of mean length (mm)
8/2/2016	Upstream #1	No data	No data	No data	No data	No data	No data
8/2/2016	Upstream #2	No data	No data	No data	No data	No data	No data
8/3/2016	Upstream #1	N/A	N/A	0	0	N/A	N/A
8/3/2016	Upstream #2	16:08:12	16:10:31	142	46.7	82.9	19
8/4/2016	Upstream #1	No data	No data	No data	No data	No data	No data
8/4/2016	Upstream #2	10:34:16	10:35:51	149	61.9	61.7	20
8/4/2016	Upstream #3	14:34:24	14:35:44	224	106.3	44.0	13
8/4/2016	Upstream #4	15:44:12	15:47:34	142	65.5	63.7	24
8/5/2016	Upstream #1	9:53:59	9:56:35	528	164.5	50.4	10
8/5/2016	Upstream #2	No data	No data	No data	No data	No data	No data
8/8/2016	Upstream #1	N/A	N/A	0	0	N/A	N/A
8/8/2016	Upstream #2	No data	No data	No data	No data	No data	No data
8/8/2016	Upstream #3	15:06:54	15:08:10	108	34.2	44.8	6
8/8/2016	Upstream #4	16:15:18	16:16:38	75	2.5	66.43	11
8/9/2016	Upstream #1	10:19:59	10:20:54	17	4.5	59.0	7
8/9/2016	Upstream #2	No data	No data	No data	No data	No data	No data
8/9/2016	Upstream #3	15:23:27	15:24:46	55	18.3	46.7	10
8/10/2016	Upstream #1	N/A	N/A	0	0	N/A	N/A
8/10/2016	Upstream #2	10:36:10	10:36:48	10	3.5	32.1	8
8/10/2016	Upstream #3	N/A	N/A	0	0	N/A	N/A
8/10/2016	Upstream #4	15:35:11	15:35:43	12	1.0	36.7	7
8/11/2016	Upstream #1	No data	No data	No data	No data	No data	No data
8/11/2016	Upstream #2	No data	No data	No data	No data	No data	No data

influenced by the tow-induced reduction in voltage gradient and by the hydrodynamics of tow movement through the confined channel. While wild fish sampling was completed immediately downstream of the EDBS, the abundance and size of fish on either side of the barrier were not fully characterized during the August 2016 field trials, though the timing of the field trials coincided with typical peak fish abundance near the EDBS (Parker et al., 2015a). Future work may address the potential impact that variations in the abundance and size of the local fish population may have on the number of fish that cross Barrier IIB during tow transits. Moreover, the DIDSON observations were limited to a small portion of the cross-section of the EDBS, and thus represent a lower bound on the number of fish that crossed Barrier IIB during each run.

Influence of the tow on the electric field

Freely swimming fish (TL < 100 mm) crossed Barrier IIB with no evidence of incapacitation during both upbound and downbound transits of the loaded tow. The ability of fish to cross an electric field without becoming incapacitated is a result of multiple biological (species-specific variation, and total length), environmental (water temperature, conductivity, and velocity), and electric field (voltage gradient, pulse width, and frequency) variables (Holliman, 2011; Holliman et al., 2015). The electric field settings of Barrier IIB were maintained throughout the experiments at 2200 V input at the electrodes, 34 Hz frequency, and 2.3 ms pulse width. While pulse width and frequency of the electric field did not change, variation was observed in the voltage gradient near the water surface due to effects of the passing tow. Fish passage was observed over the entire range of minimum voltage gradients (0.12 V/cm to 0.91 V/cm), even when the voltage gradient remained close to the baseline value. The percent reduction in voltage gradient was greater for trials in which the tow was closer to the electrical probe ($p < 0.0001$; Fig. 6), but did not correlate significantly with the number of observed fish passages ($p = 0.54$) or with the direction of tow travel through the EDBS ($p = 0.146$). Additionally, future work may assess the influence of the size and loading of a tow passing through the EDBS on the magnitude of the reduction in voltage gradient of the barrier system.

Several previous field studies and experiments have addressed the efficacy of Barrier IIA and IIB in preventing fish passage. DIDSON observations at the EDBS have shown that fish (TL = 50 mm to 180 mm) tend to accumulate downstream of the barrier, particularly near the water surface at the canal walls, and repeatedly "probe and challenge" the barrier (Parker et al., 2013, 2015a). Moreover, in the absence of a transiting tow, fish ranging in size from 50 mm to 100 mm were able to cross Barrier IIB in schools without becoming incapacitated, when the nominal operating voltage gradient was 0.91 V/cm (Parker et al., 2013). This is consistent with the present study, in which fish (TL < 100 mm; similar in size to those observed by Parker et al., 2013) crossed the high-field array of Barrier IIB only when a transiting tow caused a decrease in voltage gradient from a baseline of approximately 1.04 V/cm to a value in the range of 0.12 V/cm to 0.91 V/cm. It may be the case that the observed baseline voltage gradient (1.04 V/cm) during the present experiments was just high enough above the nominal operating voltage (0.91 V/cm) to deter the passage of small fish in the absence of tows. In another set of experiments, nearly all gizzard shad (TL 100 mm to 300 mm) were incapacitated as they were moved in a cage across Barriers IIA and IIB under nominal operating voltage gradients of 0.79 V/cm and 0.91 V/cm, respectively (Parker et al., 2015b). However, the fish in the Parker et al. (2015b) experiments were larger (TL 100 mm to 300 mm) than the fish observed in the present study (TL < 100 mm) and by Parker et al. (2013) (TL 50 mm to 100 mm), and were therefore more susceptible to the electric field (Holliman, 2011; Parker et al., 2013). Although nearly all the fish were incapacitated during the Parker et al. (2015b) experiments, the distance traveled prior to incapacitation was greater for transits near the canal wall compared to transits near the centerline, leading to the inference that the electric field is weaker near the canal walls (Parker et al., 2015b).

In addition to the measured reduction in voltage gradient induced by the presence of a tow in Barrier IIB, the tow likely distorts the orientation of the electric field because electric fields will orient to be perpendicular to the surface of a conductor (Griffiths, 1999). In the absence of a tow, the strongest component of the electric field of the barrier is oriented in the streamwise direction, such that fish swimming upstream experience the strongest voltage gradient (Holliman, 2011). As a result, fish challenging the electric barrier tend to orient their long axes mainly

Please cite this article as: Davis, J.J., et al., Effects of tow transit on the efficacy of the Chicago Sanitary and Ship Canal Electric Dispersal Barrier System, J. Great Lakes Res. (2017), http://dx.doi.org/10.1016/j.jglr.2017.08.013

in the cross-stream direction, and swim at an angle to move upstream, which minimizes exposure to the electric field (Holliman, 2011; Parker et al., 2015a). The present study is limited to analysis of the reduction in the streamwise component of the electric field at Barrier IIB. Future work may test the hypothesis that the electric field orients in the cross-stream direction alongside the tow, and vertically beneath the tow, rather than the streamwise direction, when a tow is present in the electric barrier. If this hypothesis holds true, fish swimming parallel to the side of a tow would be oriented roughly parallel to the electric field, and would not experience the strongest component voltage gradient.

Hydrodynamics of tows moving through the EDBS

Return currents generated by vessels moving in confined channels are well-documented, and several theoretical relationships exist for predicting their magnitude (Schijf, 1949; Schijf and Jansen, 1953; Constantine, 1960; Tothill, 1966; Bouwmeester, 1977; Hochstein and Adams, 1989; Maynord and Siemsen, 1991; Bhowmik et al., 1995; Das et al., 2012; Bryant et al., 2016). The magnitude of the return current depends strongly on whether or not the tow is traveling with, or against, the ambient flow velocity. The increase in streamwise velocities for upbound tows, and decrease in streamwise velocities for downbound tows, are caused by the displacement of water by the tow as it travels in a confined channel. If all else is held equal, as the width, length, and draft of a tow increase, the magnitude and duration of the return current increases, and faster tow speeds result in greater magnitude return currents that are shorter in duration. Similarly, a tow transiting in a channel with a small wetted cross-sectional area would generate a greater magnitude return current than if that same tow transited a larger channel. With the exception of the ambient flow velocity, these factors were not examined in the present study because the same general tow configuration was used in all trials, the range in tow speed and the number of trials at different speeds were not sufficient for analysis, and the area of the canal's wetted cross-section did not vary substantially across trials. Additionally, velocity measurements in the present study were limited to the area between the tow and the west canal wall, though previous work has shown that the return current is present below and on both sides of a vessel moving through a confined channel (e.g. Bhowmik et al., 1995; Das et al., 2012; Bryant et al., 2016).

DIDSON observations indicate that fish only crossed Barrier IIB by moving in the same direction as the return current, suggesting that hydrodynamics influences fish behavior during tow transits across the EDBS. Moreover, the two downbound tow transits that generated the fastest upstream (negative) return currents were the same two trials in which the largest numbers of fish crossed the barrier in the upstream direction, whereas the two downbound trials with no fish passages were the only two trials in which the ambient flow velocity was sufficient to prevent a negative (upstream) return current (Fig. 9). Although there is considerable scatter in the relation between return current velocity and number of fish passages (Fig. 9), these results suggest that the direction of the return current is a key control on the direction of fish passage across Barrier IIB. Given the propensity for fish to accumulate downstream and probe the barrier (Parker et al., 2013, 2015a), return flows induced by moving tows may result in deeper penetration of the barrier system by probing fish. Additionally, fish crossing in the same direction as the return velocity will minimize their exposure time in the electric field which reduces the likelihood of incapacitation (Parker et al., 2015b). The data collected in this study are insufficient to clearly define the detailed nature of the response of fish to the return current. However, the observations that small fish actively swim across the EDBS in the same direction as the return current during tow transits suggests that hydrodynamics influences fish behavior to some degree. Moreover, even an incapacitated fish would be moved some distance by the return current. Potential mitigation methods aimed at preventing upstream fish passage might focus on preventing flow reversal during downbound tow transits.

Implications for the efficacy of the EDBS to prevent upstream movement of bigheaded carps

Currently, the furthest upstream detection of juvenile bigheaded carps was located near RM 256.6 of the Illinois Waterway, which is approximately 63.5 km downstream of the EDBS (ACRCC Monitoring and Rapid Response Workgroup, 2015). It is therefore particularly important to examine the mechanisms for upstream fish passage across the EDBS, and to discuss potential mitigation methods in the event that juvenile bigheaded carps move further upstream. The potential for upstream transport of small fish across the EDBS in the interstitial spaces between barges of upbound tows has been previously noted (Bryant et al., 2016; Davis et al., 2016). The present study describes a mechanism in which downbound tows moving through the EDBS can facilitate upstream movement of fish across the barrier. The decrease in the voltage gradient and possible distortion of the electric field induced by transiting tows decreases the likelihood that small fish will become incapacitated in the barrier. Additionally, the data suggest that flow reversal caused by downbound tows may play a role in the likelihood of fish passage in the upstream direction across Barrier IIB (Figs. 6 & 8).

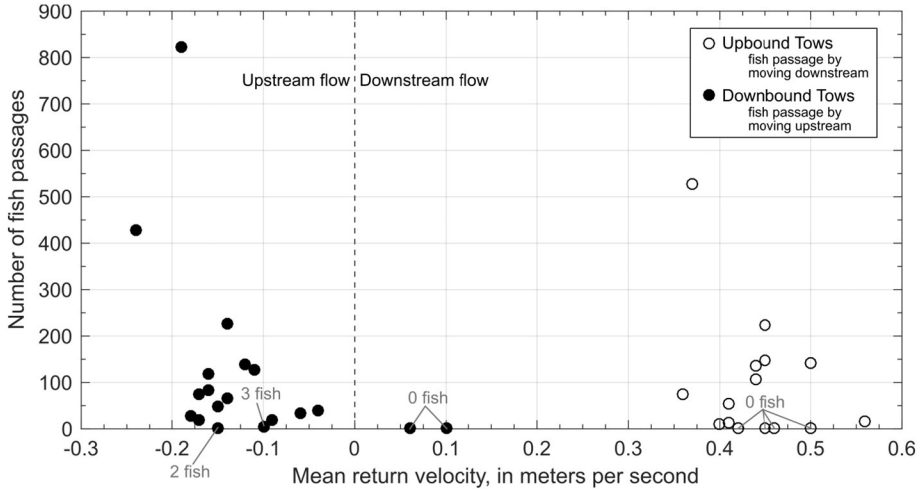

Fig. 9. Number of observed fish passages across the high field array of Barrier IIB plotted against the mean return current velocity for downbound transits of the Electric Dispersal Barrier System. Note that fish only crossed the high-field array of Barrier IIB by moving in the upstream direction during downbound tow transits, and only crossed by moving in the downstream direction during upbound tow transits.

Please cite this article as: Davis, J.J., et al., Effects of tow transit on the efficacy of the Chicago Sanitary and Ship Canal Electric Dispersal Barrier System, J. Great Lakes Res. (2017), http://dx.doi.org/10.1016/j.jglr.2017.08.013

The operating parameters of the EDBS are tuned to be effective for incapacitation of juvenile bigheaded carps (bighead carp and silver carp) (Holliman, 2011). However, similar to gizzard shad, bighead carp will repeatedly challenge an electric barrier, even after recently recovering from incapacitation (Holliman, 2011). Bighead carp will also continue to swim upstream in an electric field even after showing signs of distress (Holliman, 2011). These behavioral observations suggest that if the population front of bighead carps advanced to the EDBS, the fish would tend to accumulate downstream of the barrier system and display the same probing behavior observed by Parker et al. (2013, 2015a). As a result, the impact of tows on the electric field of the EDBS would present an increased risk of passage of juvenile bigheaded carps in the event that the bigheaded carp population front moves upstream.

Assuming that upstream return currents increase the probability of upstream fish passage, mitigation efforts may focus on preventing upstream flows. Upstream return currents may be prevented by limiting the size, draft, and speed of vessels moving downstream through the EDBS, and/or by increasing the ambient flow velocity. The present study is limited to a single tow configuration and draft, and a narrow range of tow speed. Currently, there are not sufficient data to determine if smaller tow configurations combined with slower tow speeds could completely avoid upstream return currents for the typical range of ambient flow velocities. However, it is clear that for any downbound tow of a given size and speed, a threshold ambient downstream flow velocity exists that would prevent the occurrence of upstream return currents at the EDBS. In this study, an ambient flow velocity of 0.33 m/s was sufficient to prevent an upstream return current for a downbound 2×3 tow moving at 1.3 m/s (Supplementary Table 2). Based on historical discharge data collected between 1988 and 2006 at the USGS streamflow-gaging station in the CSSC at Romeoville, IL (station number 05536995; USGS National Water Information System, http://dx.doi.org/10.5066/F7P55KJN), a mean channel velocity of 0.33 m/s is equivalent to a discharge of approximately 133 m^3/s (varies slightly depending on stage). Thus, by regulating the discharge in the Lockport Pool of the CSSC, it may be possible to prevent upstream return currents caused by tows. Further research is needed to confirm the link between upstream return currents and upstream fish passage, as well as to determine threshold ambient flow velocities for tows with different tow configurations.

Conclusions

This study has shown that the efficacy of the EDBS in preventing the passage of small, wild fish (TL < 100 mm) is compromised while tows are moving across the barrier system. These small fish were observed by DIDSON sonar to actively swim upstream, completely across the peak electric field of the Barrier IIB high-field array, during 17 out of 19 downbound transits of a loaded tow configuration. Similarly, small fish were observed to actively swim downstream, completely across the electric field of Barrier IIB high-field array, during 11 out of 15 upbound transits of a loaded tow configuration. Moreover, these schools were not observed to breach the Barrier IIB in the absence of a transiting tow during this study.

Return currents and decreases in voltage gradients induced by transiting tows likely contributed to the observed fish passage through the EDBS. In particular, downbound tows moving through the EDBS create a pathway for the upstream movement of small fish across the EDBS, and therefore may increase the risk of transfer of invasive fishes from the Mississippi River Basin to the Great Lakes Basin. The potential for further upstream movement of juvenile bigheaded carps from their current furthest upstream detection—near RM 256.6 of the Illinois Waterway, 63.5 km downstream of the EDBS (ACRCC Monitoring and Rapid Response Workgroup, 2015)—highlights the importance of continued investigation and improvement of the efficacy of current invasive species management approaches. Further research is needed to develop mitigation approaches that ensure the EDBS remains effective in preventing fish passage at all times.

Acknowledgments

This work was funded by the Great Lakes Restoration Initiative (DW-014-92450701-0). Support was provided by Will County IL Emergency Management Agency and the 9th District of the U.S. Coast Guard. The authors wish to thank the field crews of the USFWS, USGS, and USACE and the crew of the M.V. Dennis Egan for their help in conducting these logistically-complex field trials.

Disclaimer

Any use of trade, firm, or product names is for descriptive purposes only and does not imply endorsement by the U.S. Government. The findings and conclusions in this article are those of the author(s) and do not necessarily represent the views of the U.S. Fish and Wildlife Service.

Appendix A. Supplementary data

Supplementary data to this article can be found online at http://dx.doi.org/10.1016/j.jglr.2017.08.013.

References

Asian Carp Regional Coordinating Committee Monitoring and Rapid Response Workgroup, 2013. FY 2013 Asian Carp Control Strategy Framework. http://asiancarp.us/documents/2013Framework.pdf, Accessed date: 1 December 2015.

Asian Carp Regional Coordinating Committee Monitoring and Response Workgroup, 2015. Presence of Bighead and Silver Carp in Illinois Waterway. http://www.asiancarp.us/documents/map103015.pdf, Accessed date: 1 December 2015.

Bhowmik, N.G., Xia, R., Mazumder, B.S., Soong, T.W., 1995. Return flow in rivers due to navigation traffic. J. Hydraul. Eng. 121 (12), 914–918.

Bouwmeester, J., 1977. Calculation of return flow and water level depression; new method. XXIV International Navigation Congr. PIANC, Brussels, Belgium, pp. 148–151.

Bryant, D.B., Maynord, S.T., Park, H.E., Coe, L., Smith, J., Styles, R., 2016. Navigation effects on Asian carp movement past electric barrier, Chicago Sanitary and Ship Canal. U.S. Army Corps of Engineers Technical Report ERDC/CHL TR-15-X. 71 :pp. 1–57. http://hdl.handle.net/11681/21560, Accessed date: 20 February 2016.

Constantine, T., 1960. On the movement of ships in restricted waterways. J. Fluid Mech. 9, 247–256.

Das, S.N., Das, S.K., Kariya, J.N., 2012. Simulation of return flow in restricted navigation channel for barge-tow movements. Open Ocean Eng. J. 5, 34–46.

Davis, J.J., Jackson, P.R., Engel, F.L., Leroy, J.Z., Neeley, R.N., Finney, S.T., Murphy, E.A., 2016. Entrainment, retention, and transport of freely swimming fish in junction gaps between commercial barges operating on the Illinois Waterway. J. Great Lakes Res. 42:837–848. http://dx.doi.org/10.1016/j.jglr.2016.05.005.

Dettmers, J.M., Boisvert, B.A., Barkley, T., Sparks, R.E., 2005. Potential impact of steel-hulled barges on movement of fish across an electric barrier to prevent the entry of invasive carp into Lake Michigan. Illinois State Natural History Survey, Center for Aquatic Ecology, Aquatic Ecology Technical Report 2005/14, Urbana, IL.

Griffiths, D.J., 1999. Introduction to Electrodynamics. third ed. Prentice Hall, New Jersey.

Hochstein, A.B., Adams, C.E., 1989. Influence of vessel movements on stability of restricted channels. J. Waterw. Port Coast. Ocean Eng. 115, 444–465.

Holliman, F.M., 2011. Operational Protocols for Electric Barriers on the Chicago Sanitary and Ship Canal: Influence of Electrical Characteristics, Water Conductivity, Fish Behavior, and Water Velocity on Risk for Breach by Small Silver and Bighead Carp. Final Report. Smith-Root Inc., Vancouver, Washington:p. 116. http://www.lrc.usace.army.mil/Portals/36/docs/projects/ans/docs/Interim%20IIA%20with%20app%20090811.pdf, Accessed date: 13 March 2017.

Holliman, F.M., Killgore, K.J., Shea, C., 2015. Development of operational protocols for electric barrier systems on the Chicago Sanitary and Ship Canal: induction of passage-preventing behaviors in small sizes of silver carp. ANSRP Technical Notes Collection. ERDC/TN ANSRP-15-1. U.S. Army Engineer Research and Development Center, Vicksburg, MS http://hdl.handle.net/11681/5087, Accessed date: 20 February 2016.

Jackson, P.R., Johnson, K.K., Duncker, J.J., 2012. Comparison of index velocity measurements made with a horizontal acoustic Doppler current profiler and a three- path acoustic velocity meter for computation of discharge in the Chicago Sanitary and Ship Canal near Lemont, Illinois. U.S. Geological Survey Scientific Investigations Report 2011–5205 (42 pp.).

LeRoy, J.Z., Jackson, P.R., Engel, F.L., 2017. Velocity profiling at the US Army Corps of Engineers Electric Dispersal Barrier in the Chicago Sanitary and Ship Canal during passage of fully loaded commercial tows: U.S. Geological Survey data release. http://dx.doi.org/10.5066/F7K35RTP.

Maynord, S.T., Siemsen, T., 1991. Return velocities induced by shallow-draft navigation. Proc. Hydr. Div./ASCE Conf Vol. 1. ASCE, New York, NY, pp. 894–899.

Moy, P.B., Polls, I., Dettmers, J.M., 2011. The Chicago Sanitary and Ship Canal Aquatic nuisance species dispersal barrier. In: Chapman, D.C., Hoff, M.H. (Eds.), Invasive Asian carps in North America. American Fisheries Society, Symposium Vol. 74. American Fisheries Society, Bethesda, Maryland, pp. 121–137.

Parker, A.D., Rogers, P.B., Finney, S.T., Simmonds Jr., R.L., 2013. Preliminary results of fixed DIDSON evaluations at the Electric Dispersal Barrier in the Chicago Sanitary and Ship Canal. Interim Report. U.S. Fish and Wildlife Service.

Parker, A.D., Glover, D.C., Finney, S.T., Rogers, P.B., Stewart, J.G., Simmonds Jr., R.L., 2015a. Fish distribution, abundance, and behavioral interactions within a large electric dispersal barrier designed to prevent Asian carp movement. Can. J. Fish. Aquat. Sci. 73 (7):1060–1071. http://dx.doi.org/10.1139/cjfas-2015-0309.

Parker, A.D., Glover, D.C., Finney, S.T., Rogers, P.B., Stewart, J.G., Simmonds Jr., R.L., 2015b. Direct observations of fish incapacitation rates at a large electrical fish barrier in the Chicago Sanitary and Ship Canal. J. Great Lakes Res. 41 (2):396–404. http://dx.doi.org/10.1016/j.jglr.2015.03.004.

Ratcliff, E.N., Gittinger, E.J., O'Hara, T.M., Ickes, B.S., 2014. Long term resource monitoring program procedures: fish monitoring. A Program Report Submitted to the U.S. Army Corps of Engineers' Upper Mississippi River Restoration-Environmental Management Program, June 2014. Program Report LTRMP 2014-P001, 2nd edition https://pubs.usgs.gov/mis/ltrmp2014-p001/.

Schijf, J.B., 1949. Section – 1, Communication 2. XVII International Navigation Congr. PIANC, Lisbon, Portugal, pp. 61–78.

Schijf, J.B., Jansen, P.P., 1953. Section I. XVIII International Navigation Congr. PIANC, Rome, Italy, pp. 175–197.

Stockstill, R.L., Berger, R.C., 2001. Simulating barge drawdown and currents in channel and backwater areas. J. Waterw. Port Coast. Ocean Eng. 127 (5), 290–298.

Tothill, J.T., 1966. Ships in restricted channels – a correlation of model tests, field measurements, and theory. Soc. Naval Arch. and Marine Engrs, pp. 111–128.

U.S. Army Corps of Engineers, 2013. Summary of Fish-Barge Interaction Research and Fixed Dual Frequency Identification Sonar (DIDSON) Sampling at the Electric Dispersal Barrier in Chicago Sanitary and Ship Canal. http://www.lrc.usace.army.mil/Portals/36/docs/projects/ans/docs/Fish-Barge%20Interaction%20and%20DIDSON%20at%20electric%20barriers%20-%2012202013.pdf, Accessed date: 11 April 2017.

U.S. Army Corps of Engineers, 2014. Great Lakes and Mississippi River Interbasin Study. http://glmris.anl.gov/documents/docs/glmrisreport/GLMRIS_Report.pdf, Accessed date: 11 April 2017.

Please cite this article as: Davis, J.J., et al., Effects of tow transit on the efficacy of the Chicago Sanitary and Ship Canal Electric Dispersal Barrier System, J. Great Lakes Res. (2017), http://dx.doi.org/10.1016/j.jglr.2017.08.013